Solala, Iina; Driemeier, Carlos; Mautner, Andreas; Penttilä, Paavo A.; Seitsonen, Jani; Leppänen, Miika; Mihhels, Karl; Kontturi, Eero

Directed Assembly of Cellulose Nanocrystals in Their Native Solid-State Template of a Processed Fiber Cell Wall

Published in:
Macromolecular Rapid Communications

DOI:
10.1002/marc.202100092

Published: 01/06/2021

Document Version
Publisher's PDF, also known as Version of record

RESEARCH ARTICLE

Macromolecular Rapid Communications

www.mrc-journal.de

Directed Assembly of Cellulose Nanocrystals in Their Native Solid-State Template of a Processed Fiber Cell Wall

Iina Solala, Carlos Driemeier, Andreas Mautner, Paavo A. Penttilä, Jani Seitsonen, Miika Leppänen, Karl Mihhels, and Eero Kontturi**

Nanoparticle assembly is intensely surveyed because of the numerous applications within fields such as catalysis, batteries, and biomedicine. Here, directed assembly of rod-like, biologically derived cellulose nanocrystals (CNCs) within the template of a processed cotton fiber cell wall, that is, the native origin of CNCs, is reported. It is a system where the assembly takes place in solid state simultaneously with the top-down formation of the CNCs via hydrolysis with HCl vapor. Upon hydrolysis, cellulose microfibrils in the fiber break down to CNCs that then pack together, resulting in reduced pore size distribution of the original fiber. The denser packing is demonstrated by N_2 adsorption, water uptake, thermoporometry, and small-angle X-ray scattering, and hypothetically assigned to attractive van der Waals interactions between the CNCs.

1. Introduction

Assembly of nanoparticles (NPs) is a vastly researched field due to its versatile application potential in, for example, catalysis, drug delivery and detection, optical devices, batteries, and sensors.[1–4] Evidently, assembly of nanoparticles is also ubiquitous in biological systems, and understanding how such systems are constructed has fundamental implications in fields such as molecular biology and diagnostics as well as regenerative medicine.[5–8] In addition to the vast range of available materials,[9–12] a plethora of assembly types exist, including ligand-programmed self-assembly in liquid dispersion,[13,14] dynamically directed self-assembly through toggled magnetic or electrical fields,[15] and liquid phase directed self-assembly in molten state,[16] to name a few. However, the assembly of biologically derived NPs has received scant attention with respect to their synthetic counterparts despite the widespread efforts to utilize natural compounds like DNA or proteins to assist NP assembly.[17,18]

Here, we demonstrate how rod-like cellulose nanocrystals (CNCs) form and simultaneously reassemble inside a solid template, namely that of a plant fiber cell wall (**Figure 1**a), that is, the endemic base of CNCs. Produced from macroscopic cellulose fibers (Figure 1b) by acid hydrolysis, CNCs are rigid, rod-like nanoparticles generally of ≈3–20 nm in width and ≈100–500 nm in length, depending on their source.[19,20] Their applications reach far and wide, from composite technology to membranes and chiral inducers.[12] The substrate in question is a common Whatman 1 filter paper, consisting of heavily processed cotton linter fibers that have nevertheless retained the principal structure of the plant cell (Figure 1a). This type of assembly is conceptually new and different from, for example, the liquid crystal formation in CNC suspensions.[21] The ordering of CNCs takes place during

Dr. I. Solala, Dr. P. A. Penttilä, K. Mihhels, Prof. E. Kontturi
Department of Bioproducts and Biosystems
Aalto University
P.O.Box 16300, Aalto FI-00076, Finland
E-mail: iina.solala@aalto.fi; eero.kontturi@aalto.fi

Dr. C. Driemeier
Brazilian Biorenewables National Laboratory (LNBR)
Brazilian Center for Research in Energy and Materials (CNPEM)
Campinas 13083–970, Brazil

Dr. A. Mautner
Polymer and Composite Engineering (PaCE) Group, Institute of Materials Chemistry and Research
University of Vienna
Währingerstrasse 42, Vienna A-1090, Austria

Dr. P. A. Penttilä
Large Scale Structures Group
Institut Max von Laue – Paul Langevin (ILL)
71 Avenue des Martyrs – CS 20156, Grenoble F-38042, Cedex 9, France

Dr. J. Seitsonen
Nanomicroscopy Centre
Aalto University
P.O. Box 15100, Aalto FI-00076, Finland

Dr. M. Leppänen
Nanoscience Centre
University of Jyväskylä
Jyväskylä 40014, Finland

The ORCID identification number(s) for the author(s) of this article can be found under https://doi.org/10.1002/marc.202100092

DOI: 10.1002/marc.202100092

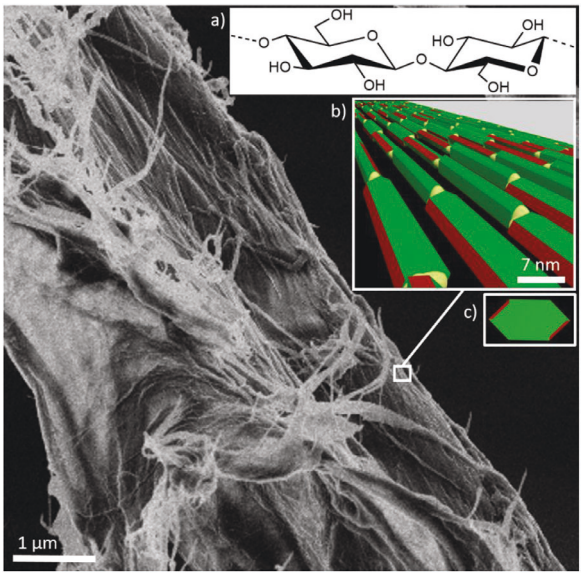

Figure 1. Cellulose (structure shown in inset (a)) fibers (here, cotton linters imaged with helium ion microscopy) consist of microfibrils with alternating crystalline and disordered regions (illustrated in inset (b) as the green/red hexagonal objects and the yellow parts between them); the latter are more reactive and can be selectively removed by acid hydrolysis. Inset (c) shows the cross-section of a single microfibril, where the red parts indicate their hydrophobic (200) planes.

their top-down generation via acid hydrolysis with hydrogen chloride vapor, that is, in a gas/solid system where CNC formation and their self-assembly occur simultaneously. This is the main difference from other reports on CNC assembly that generally rely on liquid/solid systems: CNC suspensions that can be triggered to form different solid assemblies with, for example, evaporation[21] or freezing.[22] As a result of the simultaneous formation and assembly of CNCs, a distinct change is observed in the water uptake capacity of the fibers upon the hydrolysis. The key here is to take advantage of the amphiphilic character of the cellulose crystallite (Figure 1c) where attractive van der Waals forces can be used to trigger the CNC assembly.

2. Results and Discussion

The essential step in CNC preparation involves selective chain cleavage in the disordered domains in semi-crystalline cellulose microfibrils (Figure 1b). Instead of the conventional liquid/solid system,[19] the degradation here was performed in a gas/solid setup with HCl vapor.[23,24] Despite extensive chemical degradation as evidenced by gel permeation chromatography (GPC, **Figure 2**a; Figure S1 and Table S1, Supporting Information), the hydrolyzed filter papers retained their initial macroscopic fiber structure, ostensibly showing no morphological changes, as demonstrated previously.[24] The hydrolysis actually reaches the so-called levelling-off degree of polymerization (LODP) after 24 h where all disordered regions in cellulose microfibrils have been cleaved.[24] In other words, the CNCs formed by hydrolysis were still trapped within the microfibrillar morphology of the fiber in an end-to-end connected fashion, aligned with each other. Only subsequent mechanical dispersion

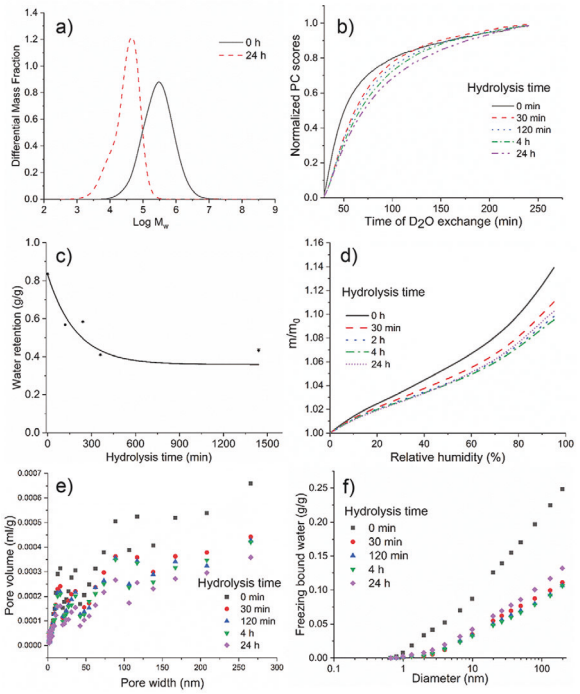

Figure 2. a) Molecular weight distributions before and after hydrolysis to leveling-off DP; all samples shown in Figure S1, Supporting Information. b) Dynamics of D_2O exchange monitored by FTIR showing that the exchange slowed down with increased hydrolysis time. Dynamics is revealed by the scores of principal component 1 (PC1) obtained by principal component analysis of the sequential FTIR spectra. c) Cellulose water retention as a function of hydrolysis time. The method is based on centrifuging a set amount of wet fiber material and weighing it before and after oven drying, yielding an estimate of the water holding capacity. d) Water vapor sorption isotherms for different hydrolysis times. e) Pore size distributions for samples hydrolyzed for different times. Both datasets determined from the N_2 adsorption isotherms. f) Freezing bound water profiles obtained by thermoporometry.

would truly individualize the CNCs.[23,24] Unexpectedly, however, the water uptake of the fibers drastically decreased as the HCl hydrolysis proceeded (Figure 2c,d), indicating that significant rearrangements had occurred with respect to the initial structure. Well in line with this interpretation, FTIR coupled with deuterium exchange and principal component analysis revealed that a single component (PC1; >97% of variance) was able to explain the dynamics of FTIR spectral change during deuterium exchange.[25] The dynamics is presented in normalized units (0 to 1) in Figure 2b. It shows that exchange is slowed down with increased hydrolysis time, indicating a slower accessibility of cellulose OH groups after the treatment.

Structural rearrangements were first characterized by nitrogen adsorption and calorimetric thermoporometry in dry and wet states, respectively. We emphasize that the mass loss during the HCl vapour hydrolysis was non-existent (in a gas/solid system) and that only 1% yield loss occurred after exposing the cellulose substrate to water following the hydrolysis. N_2 adsorption showed a decrease in specific surface area from 1.8 to 1.1 $m^2\ g^{-1}$ (Figure S2, Supporting Information). Moreover, it indicated an overall decrease of 30% in pore volume after 24 h of hydrolysis, and that half of the decrease in pore volume

Table 1. The center-to-center interfibrillar distance (*d*) as a function of hydrolysis time.

Hydrolysis time [min]	*d* [nm]
0	11.6
30	9.9
120	9.4
240	9.1
360	8.9
1440	8.6

happened already at the earliest stages of hydrolysis (first 30 min, Figure S2, Supporting Information; Figure 2e). In water-swollen conditions, thermoporometry revealed an overall decrease of 70% in the freezing bound water (FBW) already after 30 min of hydrolysis (Figure S3, Supporting Information). It is noteworthy that thermoporometry gives FBW profiles as a function of pore diameter (Figure 2f), covering two orders of magnitude in length scale (1–200 nm). Thus, it was possible to follow the development of the quantity of FBW to analyze scales smaller and larger than individual cellulose crystallite lateral dimensions (≈7 nm for the cotton linter fibers used here[26]). Interestingly, both showed a reduction in FBW (Figure 2f), demonstrating that the hydrolysis treatment reduces water uptake across multiple length scales. Similarly, the N_2 adsorption data showed an overall decrease in pore volume at different pore sizes (Figure 2e), supporting the view that structural changes had indeed occurred, and that these changes were present in both wet and dry conditions. We have recently shown that the reduction in porosity can be retained by covalent cross linking.[27]

Further indications of a structural rearrangement were derived from inverse gas chromatography (IGC), showing a minor decrease in the total surface energy and especially its acid-base component after 4 h of hydrolysis (Figure S4, Supporting Information). For additional information on changes in the microfibrillar level, small-angle X-ray scattering (SAXS) measurements were carried out in dry and wet state (Figure S5, Supporting Information). The Kratky plots enabled the calculation of the distance between microfibrils (see details in Supporting Information). **Table 1** shows that the microfibrils – or CNCs in the fully (24 h) hydrolyzed sample – came closer to each other as the hydrolysis progressed.

We postulate that the decreased water uptake and porosity as well as reduced interfibrillar distance (Figure 2, Table 1) are all an indication of microfibrillar assembly – and ultimately CNC assembly when the hydrolysis is complete after 24 h. The denser packing is hypothetically enabled by the loss of physical restraint holding the cellulose microfibrils in a strained position that occurs as the glycosidic bonds get cleaved upon hydrolysis (**Figure 3**). Since the shortened cellulose segments already exist in the immediate vicinity of each other in their native fiber template, they will now have more degrees of freedom and therefore less of a hindrance for assembling into an energetically more favorable state.

The mechanisms of the structural changes are different in large and small scales. Due to the drying step upon washing after the hydrolysis, there will be capillary forces collapsing

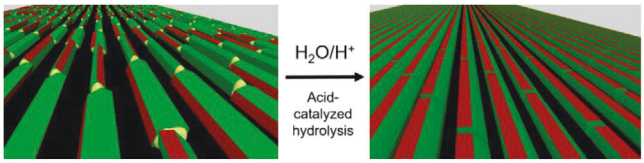

Figure 3. The proposed mechanism of CNC self-assembly within the native fiber template shown schematically.

large pores into a more compact state but drying has occurred already in the control sample (0 min hydrolysis) because of the processing of the cotton linter fibers to yield filter paper. Smaller structural changes, however, take place in the range of a couple of nanometers, that is, in a regime where attractive van der Waals forces between the (200) planes of the cellulose crystals (Figure 1) become significant.

Approximating the individual CNCs as cylinders of radius 3.5 nm, we can estimate the van der Waals interactions of two parallel CNCs (see Supporting Information). At surface-to-surface distances <2 nm, the van der Waals attraction is significantly stronger than at distances >5 nm (**Figure 4**). The interfibrillar distances estimated from SAXS data may be slightly overestimated,[28] but even as such the surface-to-surface distances between microfibrils vary between 4.6 and 1.6 nm, meaning that significant van der Waals attraction is a plausible explanation for the observed nanoscale packing. In addition to the closer packing quantitatively demonstrated by SAXS, it is possible that the nanoscopic changes also entail rotations of the released CNCs in such a way that their hydrophobic planes[29,30] turn toward one another (exaggerated illustration shown in Figure 3), thus achieving an energetically more favorable configuration, reminiscent of the assembly of Janus particles into anisotropic structures.[31,32] We point out that the scheme presented here is simplified because we have not taken into account the purported twist in CNC (or cellulose microfibrils).[33,34]

The described directed assembly system for CNCs is unique in that it takes place in solid state within a 3D plant fiber template. Reports on templated NP assemblies utilizing solid substrates

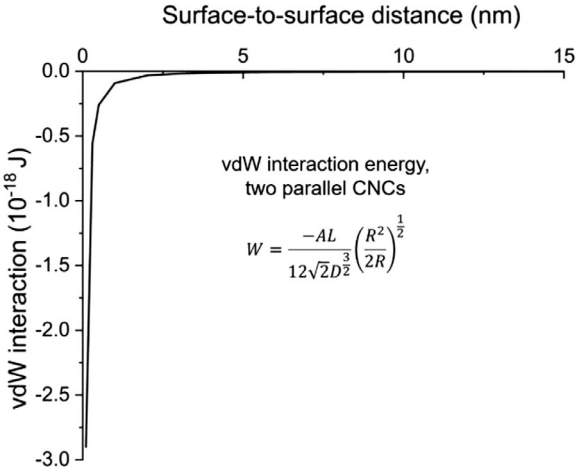

Figure 4. Calculated van der Waals interaction energy for two cylinder-like parallel CNCs of identical dimensions.

of various geometries have been reported,[35–38] but they rely on liquid media to proceed, such as in the cases of organic solid–solid wetting deposition[39] or self-templating assembly of viral particles[40] that have certain morphological similarities with our CNC system.

3. Conclusions

In summary, we report that the preparation of cellulose nanocrystals by HCl vapor in a native fiber template results in directed assembly (tighter packing) of the in situ formed nanoparticles, and that these changes significantly affect the water holding capacity of the material. Porosity and accessibility measurements as well as SAXS all confirm a denser packing of cellulose across multiple length scales, ranging from ≈2 nm to hundreds of nanometers. Densification in the nano-regime was hypothetically attributed to attractive van der Waals forces between parallel CNCs.

Supporting Information

Supporting Information is available from the Wiley Online Library or from the author.

Acknowledgements

I.S. thanks The Academy of Finland (grant no. 300364) for funding this work. C.D. acknowledges funding from FAPESP (grant 13/07932-6). P.A.P. thanks the Emil Aaltonen Foundation and Academy of Finland (grant no. 315768) for funding and ESRF for beamtime at beamline D2am (experiment 02-01-885). Rita Hatakka is acknowledged for her assistance with the GPC measurements. Work of M.L. was supported by the Jane and Aatos Erkko Foundation. The work is a part of the FinnCERES Bioeconomy ecosystem.

Conflict of Interest

The authors declare no conflict of interest.

Data Availability Statement

Research data are not shared.

Keywords

acid hydrolysis, bio-based materials, cellulose, nanoparticle assembly, porosity

Received: February 11, 2021
Revised: March 24, 2021
Published online: May 6, 2021

[1] C. Noguez, A. Sánchez-Castillo, F. Hidalgo, *J. Phys. Chem. Lett.* **2011**, *2*, 1038.
[2] K. Sztandera, M. Gorzkiewicz, B. Klajnert-Maculewicz, *Mol. Pharmaceutics* **2019**, *16*, 1.
[3] L. Peng, Z. Fang, J. Li, L. Wang, A. M. Bruck, Y. Zhu, Y. Zhang, K. J. Takeuchi, A. C. Marschilok, E. A. Stach, *ACS Nano* **2018**, *12*, 820.
[4] D. Luo, X. Qin, Q. Song, X. Qiao, Z. Zhang, Z. Xue, C. Liu, G. Mo, T. Wang, *Adv. Funct. Mater.* **2017**, *27*, 1701982.
[5] R. Pugliese, F. Gelain, *Trends Biotechnol.* **2017**, *35*, 145.
[6] A. B. Chinen, C. M. Guan, J. R. Ferrer, S. N. Barnaby, T. J. Merkel, C. A. Mirkin, *Chem. Rev.* **2015**, *115*, 10530.
[7] C. He, D. Liu, W. Lin, *Chem. Rev.* **2015**, *115*, 11079.
[8] P. D. Howes, R. Chandrawati, M. M. Stevens, *Science* **2014**, *346*, 1247390.
[9] H.-Y. Lee, S. H. R. Shin, A. M. Drews, A. M. Chirsan, S. A. Lewis, K. J. Bishop, *ACS Nano* **2014**, *8*, 9979.
[10] W. van der Stam, A. P. Gantapara, Q. A. Akkerman, G. Soligno, J. D. Meeldijk, R. van Roij, M. Dijkstra, C. de Mello Donega, *Nano Lett.* **2014**, *14*, 1032.
[11] H. Liu, T. Ye, C. Mao, *Angew. Chem., Int. Ed.* **2007**, *46*, 6473.
[12] E. Kontturi, P. Laaksonen, M. B. Linder, Nonappa, A. H. Groschel, O. J. Rojas, O. Ikkala, *Adv. Mater.* **2018**, *30*, 1703779.
[13] R. M. Choueiri, E. Galati, H. Thérien-Aubin, A. Klinkova, E. M. Larin, A. Querejeta-Fernández, L. Han, H. L. Xin, O. Gang, E. B. Zhulina, *Nature* **2016**, *538*, 79.
[14] Q. Yu, X. Zhang, Y. Hu, Z. Zhang, R. Wang, *ACS Nano* **2016**, *10*, 7485.
[15] Z. M. Sherman, J. W. Swan, *ACS Nano* **2016**, *10*, 5260.
[16] J. Fowlkes, N. Roberts, Y. Wu, J. A. Diez, A. G. González, C. Hartnett, K. Mahady, S. Afkhami, L. Kondic, P. Rack, *Nano Lett.* **2014**, *14*, 774.
[17] S. Julin, A. Korpi, B. Shen, V. Liljeström, O. Ikkala, A. Keller, V. Linko, M. A. Kostiainen, *Nanoscale* **2019**, *11*, 4546.
[18] J. Xie, L. Mei, K. Huang, Y. Sun, A. Iris, B. Ma, Y. Qiu, J. Li, G. Han, *Nanoscale* **2019**, *11*, 6136.
[19] Y. Habibi, L. A. Lucia, O. J. Rojas, *Chem. Rev.* **2010**, *110*, 3479.
[20] D. Klemm, F. Kramer, S. Moritz, T. Lindström, M. Ankerfors, D. Gray, A. Dorris, *Angew. Chem., Int. Ed.* **2011**, *50*, 5438.
[21] J. P. Lagerwall, C. Schütz, M. Salajkova, J. Noh, J. H. Park, G. Scalia, L. Bergström, *NPG Asia Mater* **2014**, *6*, e80.
[22] F. Jiang, Y.-L. Hsieh, *Carbohydr. Polym.* **2013**, *95*, 32.
[23] M. Lorenz, S. Sattler, M. Reza, A. Bismarck, E. Kontturi, *Faraday Discuss.* **2017**, *202*, 315.
[24] E. Kontturi, A. Meriluoto, P. A. Penttilä, N. Baccile, J. M. Malho, A. Potthast, T. Rosenau, J. Ruokolainen, R. Serimaa, J. Laine, *Angew. Chem., Int. Ed.* **2016**, *55*, 14455.
[25] C. Driemeier, F. M. Mendes, L. Y. Ling, *Carbohydr. Polym.* **2015**, *127*, 152.
[26] R. P. Oliveira, C. Driemeier, *J. Appl. Crystallogr.* **2013**, *46*, 1196.
[27] P. Spiliopoulos, I. Solala, T. Pääkkönen, J. Seitsonen, B. van Bochove, J. V. Seppälä, E. Kontturi, *Macromol. Rapid Commun.* **2020**, *41*, 2000201.
[28] T. Virtanen, P. A. Penttilä, T. C. Maloney, S. Grönqvist, T. Kamppuri, M. Vehviläinen, R. Serimaa, S. L. Maunu, *Cellulose* **2015**, *22*, 1565.
[29] I. Kalashnikova, H. Bizot, B. Cathala, I. Capron, *Biomacromolecules* **2012**, *13*, 267.
[30] A. N. Fernandes, L. H. Thomas, C. M. Altaner, P. Callow, V. T. Forsyth, D. C. Apperley, C. J. Kennedy, M. C. Jarvis, *Proc. Natl. Acad. Sci. U.S.A.* **2011**, *108*, E1195.
[31] W.-H. H. Yi-Cheng Chao, K.-M. Cheng, C. Kuo, *ACS Appl. Mater. Interfaces* **2014**, *6*, 4338.
[32] A. T. Kyle Miller, S. M. Anthony, S. Qin, X. Yong, S. Jiang, *Soft Matter* **2018**, *14*, 6793.
[33] I. Usov, G. Nyström, J. Adamcik, S. Handschin, C. Schütz, A. Fall, L. Bergström, R. Mezzenga, *Nat. Commun.* **2015**, *6*, 7564.
[34] K. Conley, M. A. Whitehead, T. G. M. van de Ven, *Cellulose* **2016**, *24*, 479.
[35] L. Zhou, Y. Tan, J. Wang, W. Xu, Y. Yuan, W. Cai, S. Zhu, J. Zhu, *Nat. Photonics* **2016**, *10*, 393.
[36] J. Wang, J. Liu, D. Chao, J. Yan, J. Lin, Z. X. Shen, *Adv. Mater.* **2014**, *26*, 7162.

[37] Q. Zhang, Y. H. Lee, I. Y. Phang, C. K. Lee, X. Y. Ling, *Small* **2014**, *10*, 2703.
[38] I. Choi, H. D. Song, S. Lee, Y. I. Yang, T. Kang, J. Yi, *J. Am. Chem. Soc.* **2012**, *134*, 12083.
[39] A. Eberle, T. Markert, F. Trixler, *J. Am. Chem. Soc.* **2018**, *140*, 1327.
[40] W.-J. Chung, J.-W. Oh, K. Kwak, B. Y. Lee, J. Meyer, E. Wang, A. Hexemer, S.-W. Lee, *Nature* **2011**, *478*, 364.

